

PACS numbers: 51.50.+v; 43.28.Mw; 42.55.Lt
DOI: 10.1070/QE2006v036n07ABEH013172

Self-sustained volume discharge in SF_6-based gas mixtures upon the development of shock-wave perturbations of the medium initiated by a pulsed CO_2 laser

A.A. Belevtsev, S.Yu. Kazantsev, I.G. Kononov, K.N. Firsov

***Abstract*. A self-sustained volume discharge in SF_6 mixtures with C_2H_6, He, and Ne preliminarily irradiated by CO_2 laser pulses was investigated. The radiation energy density absorbed by SF_6 in the discharge ignition region amounted to 6.5 J atm^{-1} cm^{-3}. The discharge structure and the current distribution in the discharge gap were found to change radically with increasing the time delay between the laser and discharge pulses. In particular, brightly glowing narrow channels are formed at the boundary of the irradiation region. The observed effect is shown to arise from the development of a shock-wave process due to a temperature jump at the boundary between the irradiated and unirradiated gas. The velocities of shock wave propagation and the main thermodynamic gas parameters in the perturbation region were calculated. A comparison was made between the calculated and measured velocities of the shock waves.**

Keywords: *CO_2 laser, nonchain HF laser, self-sustained volume discharge, electronegative gases, shock waves.*

1. Introduction

The interest in the study of a self-sustained volume discharge (SSVD) at medium pressures of SF_6 and its mixtures with different donors of hydrogen and deuterium is largely stimulated by the progress in the development of high-power nonchain electric-discharge chemical HF (DF) lasers, where these gases serve as the initial components for the production of active media [1 – 3]. At present, the SSVD has been realised in nonchain HF (DF) lasers with volumes of the active medium of several tens of litres [4]. However, the theoretical notions of the principal mechanisms of initiation and maintenance of such a discharge call for a substantial development.

The main distinguishing feature of a SSVD in SF_6-based gas mixtures is its development in the form of a self-initiated volume discharge, i.e. a volume discharge without preionisation of the medium [5]. This form of a SSVD can exist in strongly electronegative gases due to the effect of current density limitation in diffuse channels, which grow from cathode spots towards the anode to form, when they overlap, a volume discharge uniform throughout the gap [4, 5]. However, the relative role of different mechanisms of current density limitation in a diffuse channel (dissociation of SF_6 and other components of the mixture, electron – ion recombination, electron attachment to vibrationally excited SF_6 molecules [6]) is not yet entirely known. In this case, least understood is the role of vibrational excitation in SF_6.

To study the effect of electron attachment to vibrationally excited SF_6 molecules on the properties of SSVD in SF_6 and SF_6 mixtures with C_2H_6, in Ref. [7] we irradiated the discharge gap by pulsed CO_2-laser radiation prior to the application of a high-voltage pulse across the gap. This enabled obtaining a high degree of population of the vibrational states of the SF_6 molecule unattainable under the conditions of an electric discharge in the absence of irradiation, when no more than 2 % of the electric energy introduced into the gas-discharge plasma goes into the vibrational excitation of SF_6 [8]. It was found that the increase in electron losses through the attachment due to excitation of vibrational SF_6 states leads to a substantial (up to 30 %) increase in SSVD operating voltage, depending on the ratio between the partial pressures of the $SF_6 - C_2H_6$ mixture components, the radiation energy supplied into the gas, and the time delay between the laser and discharge voltage pulses. As a consequence of this effect, placing different diaphragms and screens in the laser beam resulted in the SSVD displacement to the region of the shadow produced by the screen, where the electron attachment was weaker and therefore the operating discharge voltage was lower than in the irradiated region.

In the experiments of Ref. [7], the energy density of laser radiation absorbed by SF_6 in the SSVD development region amounted to 6 J atm^{-1} cm^{-3}. According to our estimates, the temperature of the gas heated during the VT relaxation may exceed 1000 K for such energy inputs into the vibrational degrees of freedom of the SF_6 molecule, which should give rise to appreciable gas dynamic perturbations of the medium. In particular, because the gas density in the irradiation region remains virtually invariable during the laser pulse, this temperature jump entails the corresponding pressure jump and may be responsible for the formation of a shock wave at the boundary of the irradiation region. It would appear reasonable that this would affect the structure of the SSVD initiated upon laser irradiation of the discharge gap. However, no effect of laser-induced gas dynamic perturbations on the SSVD development was observed in

A.A. Belevtsev Institute for High Energy Densities, Associated Institute for High Temperatures, Russian Academy of Sciences, ul. Izhorskaya 13/19, 127412 Moscow, Russia; e-mail: baa@hedric.msk.su;
S.Yu. Kazantsev, I.G. Kononov, K.N. Firsov A.M. Prokhorov General Physics Institute, Russian Academy of Sciences, ul. Vavilova 38, 119991 Moscow, Russia; e-mail: kazan@kapella.gpi.ru

Received 31 March 2006
Kvantovaya Elektronika **36** (7) 646 – 652 (2006)
Translated by E.N. Ragozin

Ref. [7]. This can be explained by the fact that the change of SSVD structure in the preliminarily irradiated gap was investigated in Ref. [7] for too short a time delay between the high-voltage and laser pulses, which did not exceed the duration of the latter. As a consequence, by the instant of SSVD initiation, either part of the laser energy introduced into the gas went into heat or the shock-wave perturbation resulting from the temperature jump did not manage to redistribute the gas density in the gap to such a degree that it could distinctly manifest itself in the discharge structure.

In this work, we investigate the SSVD development in SF_6 mixtures with ethane, helium, or neon preliminarily irradiated by a CO_2 laser pulse; in doing this we vary the delay times and the pressures of the mixture components over a wide range.

2. Experimental setup and experimental technique

The experimental setup and technique were similar to those described in Refs [7, 9]. A SSVD was initiated in $SF_6-C_2H_2-He$ (Ne) gas mixtures with partial component pressures $p_{SF_6} = 15$ Torr, $p_{C_2H_6} = 3$ Torr, and $p_{He,Ne} = 0 - 30$ Torr, which were preliminarily irradiated by the pulse of a TEA CO_2 laser operating at the P(20) line of the 10.6-μm band. The spatially uniform laser beam with a total transverse dimension of 50×60 mm was directed into the discharge chamber through a BaF_2 window. The energy density W_a of laser radiation absorbed by SF_6 in the region of discharge development was $0.1 - 0.13$ J cm^{-3}. The W_a measuring technique is described in detail in Refs [9, 10].

The SSVD was initiated in the gap between a needle (the cathode) and a cylinder 15-mm in diameter (the anode) for an interelectrode distance of 43 mm. The needle was directed perpendicular to the cylinder axis, which in turn was perpendicular to the direction of the laser beam introduced into the discharge chamber. The function of the needle was fulfilled by a length of copper wire 1.5 mm in diameter with a polyethylene insulation, which did not allow the discharge to develop from the side cathode surface. A capacitor with a 2.5-nF capacitance charged to 24 kV discharged into the gap. The total duration of the SSVD current through the unirradiated gap was $\tau_d \approx 275$ ns.

The pulse of voltage U_{las} was applied across the gap with a variable time delay $\tau = 0 - 40$ μs relative to the laser pulse P_{las}. For ease of understanding of the subsequent material, Fig. 1 shows the oscillograms of P_{las} and U_{las}. One can see that the laser pulse has a shape which is typical for CO_2 lasers with a transverse discharge, its total duration being $\tau_{las} \approx 3$ μs. Note that the time τ is measured from the onset of the leading edge of the laser pulse.

To monitor changes in the SSVD structure caused by irradiation of the gas, the gap was photographed with a digital camera through the window of the discharge chamber located oppositely to the entrance window. The gap irradiation profile was defined by a diaphragm and a screen, which are depicted respectively in Figs 2a and 2b, mounted in front of the entrance window. Figure 2c shows a photograph of the SSVD in the unirradiated gap. One can see that the SSVD in the absence of irradiation possesses a form typical for the geometry involved: its transverse dimension increases in the direction from the cathode towards the anode to attain a value of ~ 29 mm at the anode. In the case when a diaphragm measuring

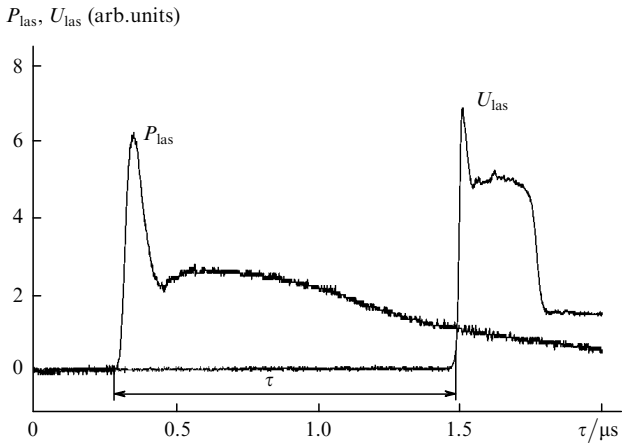

Figure 1. Oscillograms of the voltage pulses U_{las} across the SSVD plasma and laser radiation P_{las}.

50×35 mm is placed in front of the entrance window of the discharge chamber, the laser beam completely spans the discharge gap region in which the SSVD operates in the absence of irradiation. When the screen was placed in the beam, the entire gap is irradiated with the exception of a 10-mm wide strip in its central part. It is worthy of note that in either case the dimension of irradiated region in the cathode–anode direction exceeds the electrode separation.

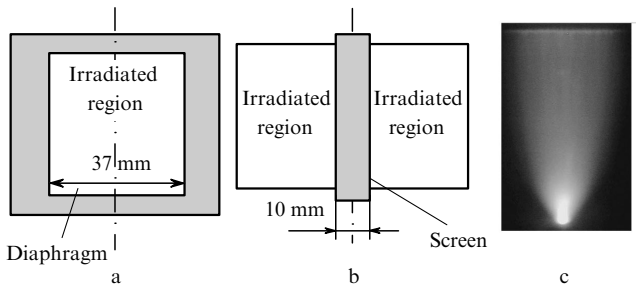

Figure 2. Discharge gap profiles determined by a diaphragm (a) and a screen (b) and photograph of the SSVD in the unirradiated gap (c).

We recorded the oscillograms of the SSVD voltage and current for each value of τ as well as in the absence of pulsed laser irradiation of the gap. The increase in the losses of electrons due to their attachment to vibrationally excited laser-irradiated SF_6 molecules, which manifests itself, as noted above, in the increase in the SSVD operating voltage, was characterised by the parameter $\Delta = (U_{las} - U_d)/U_d$, where U_{las} and U_d are the operating voltages in the irradiated and unirradiated gap, respectively. For definiteness, U_{las} and U_d were measured at the maxima of the corresponding currents. When recording the dependences of Δ on τ given below, the beam was not diaphragmed, i.e. its transverse dimension (60 mm) significantly exceeded the transverse discharge dimension at the anode.

3. Experimental results

Figure 3 shows the dependences $\Delta(\tau)$ recorded for the mixtures of composition $SF_6 : C_2H_6 = 5 : 1$, $SF_6 : C_2H_6 : He = 5 : 1 : 5$ and $5 : 1 : 10$ without diaphragming the laser beam. For each mixture one can distinguish three

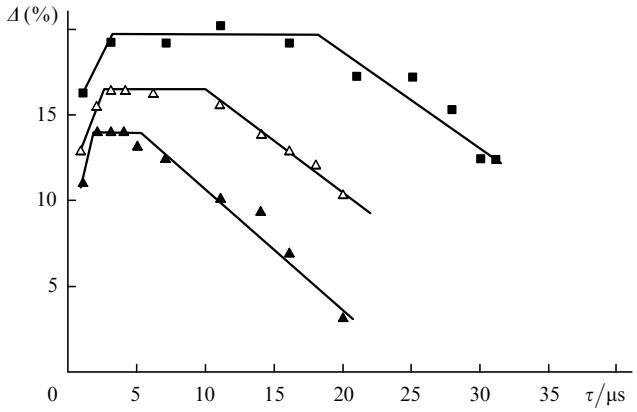

Figure 3. Dependence of the parameter Δ on the time delay τ between the laser and discharge pulses for the mixtures of composition $SF_6 : C_2H_6 = 5 : 1$ (■), $SF_6 : C_2H_6 : He = 5 : 1 : 5$ (△) and $5 : 1 : 10$ (▲); $W_a = 0.13$ J cm^{-3} for $\tau > 3$ μs.

characteristic parts of the curves. In the first part, Δ increases with τ to attain its maximum for $\tau \approx 3$ μs. The second part is a rather lengthy 'shelf', where the value of Δ virtually coincides with the maximum value. In the third part, Δ noticeably decreases with τ, this decrease beginning much earlier in He-containing mixtures compared to the mixture from which this component is missing. The increase of Δ in the first part, which approximately coincides in length with the quantity τ_{las}, is due to the growth of the populations of SF_6 vibrational states with increasing laser energy absorbed by the gas. The underlying reasons for the emergence of two other parts of the $\Delta(\tau)$ curve are less evident. In particular, one might assume that the decrease of Δ for long τ is due to the VT relaxation of the vibrational states of the SF_6 molecule, which is responsible for a lowering of their populations and therefore for a lowering of the electron losses due to attachment to vibrationally excited SF_6 molecules. However, even the knowingly exaggerated estimates of VT relaxation times τ_{VT}, which are made without the inclusion of gas heating and under the assumption that the SF_6 molecule relaxes in collisions with only one component of the mixture, yield values which are significantly shorter than the 'shelf' lengths in Fig. 3. Indeed, using the data of Ref. [11] we obtain $\tau_{VT} = 8.1$, 2.1, and 1.2 μs for the mixtures of composition $SF_6 : C_2H_6 = 5 : 1$, $SF_6 : C_2H_6 : He = 5 : 1 : 5$ and $5 : 1 : 10$, respectively. That is why other reasons should be sought to account for the decrease of Δ for long τ.

An analysis of the SSVD photographs made in the case of gap irradiation by the undiaphragmed beam showed that, in parallel with the main discharge, in the region under irradiation there develops a brighter and narrower channel at the boundary of the irradiation region for values of τ that correspond to the parts of Δ decrease in Fig. 3. Consequently, the lowering of Δ for long τ may arise from current redistribution in the gap accompanied with the formation of channels with a higher conductivity than the main discharge. To verify this assumption, the boundary of the irradiation region had to be brought closer to the region of the main discharge in order to shorten the region in which the channel developed and accordingly to produce the conditions that were favourable to its formation. This was achieved by shortening the transverse laser beam dimension with a diaphragm.

Figure 4 shows the photographs of discharge in the mixture of composition $SF_6 : C_2H_6 : He = 5 : 1 : 5$ taken for different values of τ under the specified conditions. From these data it follows that irradiation leads to a substantial change in the SSVD form. Even for $\tau = 1$ μs, when the laser energy has not been completely supplied into the gas, the

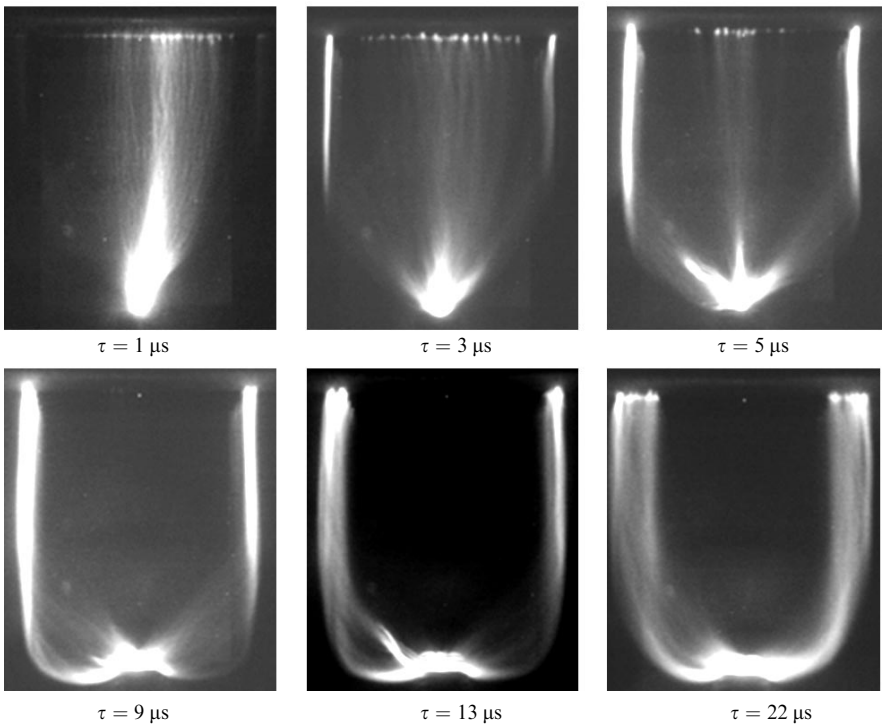

Figure 4. Photographs of the SSVD in the mixture of composition $SF_6 : C_2H_6 : He = 5 : 1 : 5$ for different τ. Irradiation was effected through a diaphragm; $W_a = 0.13$ J cm^{-3} for $\tau > 3$ μs.

transverse discharge dimension at the anode is significantly greater than in the unirradiated gap, the discharge as if tends to escape from the irradiation region (see Fig. 2 for comparison). Also observed is the filamentary structure typical for the SSVD discharge in vibrationally excited SF_6 [7, 9]. For $\tau = 3$ μs, at the boundary of irradiation region there appear narrow, brightly glowing channels ('whiskers'), whose brightness increases with τ for a simultaneous lowering of SSVD brightness in the irradiation region.

For $\tau \geqslant 9$ μs, the discharge is completely beyond the irradiation region, skirting it along the boundaries even at the cathode, where the current streamlines become almost perpendicular to the central line of the electrostatic field, which corresponds to the gap geometry. This picture outwardly resembles the development of a sliding discharge along the surface of a solid dielectric introduced into the gap. The surface over which the discharge slides in this case is the boundary of gas irradiation region. The 'whiskers' at this boundary are, despite their relatively high brightness, diffuse in nature as demonstrated by the oscillograms of current and voltage, which are typical for volume discharges even for long τ. It is worthy of note that decreasing the transverse beam dimension with a diaphragm makes the 'shelf' in the dependences $\Delta(\tau)$ disappear, so that Δ begins to decrease with τ immediately after reaching its peak ($\tau \approx 3$ μs) to become negative for $\tau > 5 - 10$ μs (depending on the mixture composition).

Therefore, the photographs shown in Fig. 4 testify that the decrease of Δ for long τ may be related to the geometric factor, specifically to the redistribution of current density over the gap and to the escape of the discharge from the irradiation region to its boundaries. In this case, the length of current streamlines is far greater than the minimal interelectrode distance. It is therefore believed that in this case the discharge (the 'whiskers') develops, at least partly, in a rarefied gas. The occurrence of the rarefaction region may be related to the formation and propagation of a shock wave due to the temperature jump at the boundary of irradiation region.

To verify this assumption, we investigated the SSVD with the beam profile defined by the screen. Figures 5 and 6 show the SSVD photographs for different τ, which were taken in the $SF_6 : C_2H_6 = 5 : 1$ and $SF_6 : C_2H_6 : He = 5 : 1 : 10$ mixtures, respectively, with the irradiation profile defined in this way. One can see that for $\tau = 1 - 2$ μs the SSVD operates only in the region of the shadow produced by the screen, in the form of a virtually rectangular strip (with the exception of the cathode region). Unlike the discharge in a vibrationally excited gas, the SSVD exhibits a clearly defined diffuse character, the filamentary structure is absent.

With lengthening τ, the width of diffuse strip decreases, and near the boundary of irradiation region there appear, like in Fig. 4, brightly glowing 'whiskers' separated from the initial diffuse discharge by narrow dark strips. In He-containing mixtures, the 'whiskers' are formed for shorter τ than in the helium-free mixture. On further increase of τ, the width of the diffuse strip and the brightness of its glow decrease for a simultaneous rise in glow brightness of the 'whiskers' and a broadening of the region they occupy. For $\tau \geqslant 9$ μs in the case of the $SF_6 - C_2H_6$ mixture and for $\tau \geqslant 7$ μs in the case of the $SF_6 - C_2H_6 - He$ mixture, the diffuse strip becomes indistinguishable in the photographs, the discharge current transfers to the 'whiskers' completely.

Therefore, when the laser beam profile is defined by the screen, the current redistribution over the gap with lengthening τ is also observed. This redistribution testifies to the

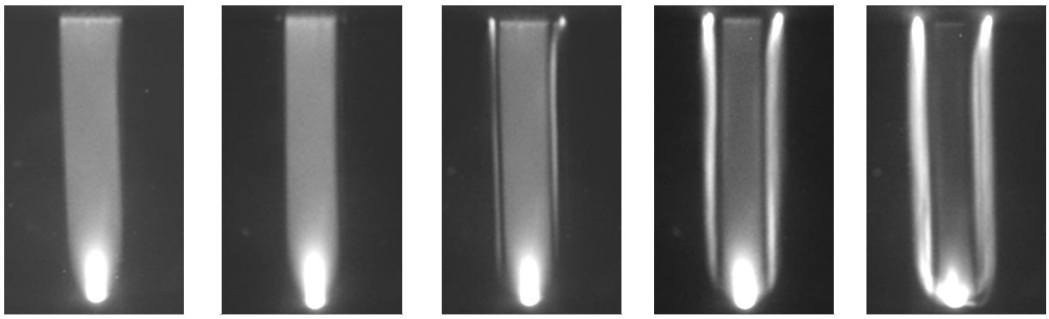

$\tau = 1$ μs $\tau = 3$ μs $\tau = 4$ μs $\tau = 7$ μs $\tau = 9$ μs

Figure 5. Photographs of the SSVD in the mixture of composition $SF_6 : C_2H_6 = 5 : 1$ for different τ. A screen is placed in the laser beam; $W_a = 0.13$ J cm^{-3} for $\tau > 3$ μs.

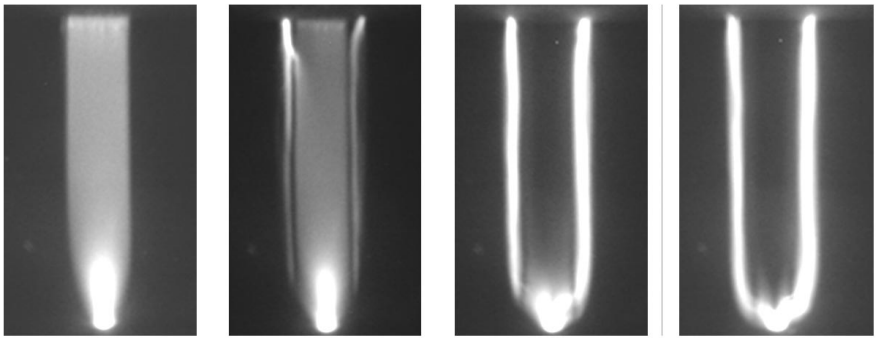

$\tau = 1$ μs $\tau = 3$ μs $\tau = 5$ μs $\tau = 7$ μs

Figure 6. Photographs of the SSVD in the mixture of composition $SF_6 : C_2H_6 : He = 5 : 1 : 10$ taken for the same irradiation conditions as in Fig. 5.

formation of gas rarefaction and compression regions most likely caused by the emergence and propagation of a shock wave due to a temperature jump at the boundary of irradiation region. The displacement of the shock front in time is indicated by the position of the edge of diffuse discharge strip in Figs 5 and 6, and the dependence of the transverse dimension H of the diffuse strip on τ permits measuring the shock velocity V_{sh}. Figure 7 shows these dependences for some of the mixtures investigated.

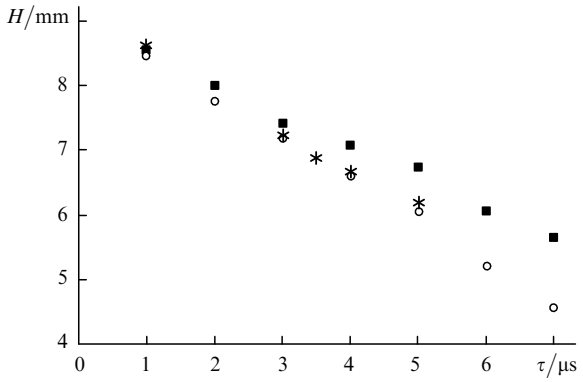

Figure 7. Transverse dimension H of a diffuse discharge region as a function of τ for the mixtures of composition $SF_6 : C_2H_6 = 5 : 1$ (■), $SF_6 : C_2H_6 : He = 5 : 1 : 5$ (∗), and $SF_6 : C_2H_6 : Ne = 5 : 1 : 10$ (○); $W_a = 0.11$ J cm^{-3} for $\tau > 3$ μs.

4. Discussion of results

4.1 Thermodynamic gas parameters in the irradiation region

The relaxation of laser radiation energy absorbed by SF_6 molecules was discussed in detail in our earlier paper [10]. We showed, in particular, that the characteristic times of intramode (τ_{VV}) and intermode ($\tau_{VV'}$) vibrational energy exchange in SF_6 for a partial pressure $p_{SF_6} = 15$ Torr do not exceed 70 ns. Under the 'thermal explosion' theory approximation, we also estimated the time required for the establishment of equilibrium between the vibrational and translational degrees of freedom as a result of VT relaxation. In this case, use was made of the dependence of the characteristic VT relaxation time on the gas temperature T_g recommended in Ref. [12]:

$$\tau_{VT}(T_g) = \tau_{VT}(T_0/T_g)^{\alpha}, \quad \alpha \gg 1, \tag{1}$$

where τ_{VT} is taken for the cold gas temperature $T_0 \approx 300$ K. Other $\tau_{VT}(T_g)$ approximations, for instance the Landau–Teller one [12, 13], may appreciably differ from expression (1) only for relatively high T_g values, when the thermodynamic equilibrium in the gas is already established. In this case, however, consideration of the relaxation times becomes unnecessary at all. Proceeding from the results of Ref. [10], the expression for the vibrational–translational temperature equalisation time τ_{exp} can be written as

$$\tau_{exp} = \left[\frac{2C_V(T_0)T_0N\tau_{VT}\tau_{las}}{(\alpha-1)W_a}\right]^{1/2}. \tag{2}$$

Here, $C_V(T_0)$ is the initial heat capacity of the gas mixture at constant volume per particle; N is the total gas particle density. Relationship (2) was obtained ignoring the difference between the τ_{VT} values for SF_6 and C_2H_6 as well as the vibrational energy exchange between these components, because the relative ethane density is low. That is why in Ref. [10], where inert gases were absent from the mixtures under investigation ($SF_6 - C_2H_6$ mixtures with a relatively low content of C_2H_6), the values of C_V and N could be attributed exclusively to the SF_6 molecules when considering the relaxation.

Let us estimate the time τ_{exp} by putting $\alpha = 5$. Proceeding from relationship (2), the data on τ_{VT} borrowed from Ref. [11], and the data from [14, 15] on the heat capacities for the components of the mixtures under investigation, for $W_a = 0.13$ J cm^{-3} we obtain $\tau_{exp} \approx 1.5$, 0.9, and 0.7 μs for the mixtures of composition $SF_6 : C_2H_6 = 5 : 1$, $SF_6 : C_2H_6 : He = 5 : 1 : 5$ and $5 : 1 : 10$, respectively. In view of the aforesaid about the times τ_{VV} and $\tau_{VV'}$, we can assert, despite some uncertainty in the magnitude of α, that the gas in the irradiation region will be in the state of thermodynamic equilibrium by the time of completion of the laser pulse ($\tau_{las} \approx 3$ μs).

It is significant that the appreciable gas heating begins only from the instant $t \approx \tau_{exp}$ due to the explosive character of temperature increase [10]. In the determination of the temperature T that sets in upon completion of the laser pulse, this permits resorting to the equilibrium values of heat capacity without introducing errors of any significance, the more so as the corresponding relation is given by an integral relationship. Furthermore, taking into account that the total density of the gas and its chemical composition are hardly changed during the laser pulse (τ_{las}), according to our estimates, we obtain

$$\frac{W_a}{N} = \int_{T_0}^{T} C_V(T')\mathrm{d}T', \quad C_V(T') = \sum_i \xi_i C_{Vi}(T'). \tag{3}$$

Summation in expression (3) is performed over all components of the gas mixture; ξ_i is the initial relative density of the ith component. The following simple relationships are valid for the adiabatic exponent γ and the sound velocity V_s provided that the composition remains invariable:

$$\gamma = 1 + \frac{R}{C_V(T)}, \quad V_s = \left(\gamma\frac{RT}{\mu}\right)^{1/2}, \quad \mu = \sum_i \xi_i\mu_i. \tag{4}$$

Here, μ_i is the molecular weight of the ith component of the mixture; R is the universal gas constant. Table 1 shows the values of γ and V_s for some of the mixtures under investigation, which were calculated according to expressions (3) and (4) for the initial gas temperature $T_0 = 300$ K and $W_a = 0.11$ J cm^{-3}. The $C_V(T)$ dependences for SF_6 and C_2H_6 were obtained with the use of the data of Ref. [15] for the heat capacities $C_p(T)$ of these gases at constant pressure. Also given for comparison in Table 1 are the values of γ_0 and V_{s0} in the unirradiated gas. Note that the calculated values of the temperature T under the

Table 1. Values of T, γ, V_s, γ_0, and V_{s0} for $T_0 = 300$ K and $W_a = 0.11$ J cm^{-3} for different mixtures.

Mixture composition	T/K	γ	V_s/m s^{-1}	γ_0	V_{s0}/m s^{-1}
$SF_6 : C_2H_6 = 5 : 1$	1240	1.06	294.9	1.10	146
$SF_6 : C_2H_6 : He = 5 : 1 : 5$	1175	1.10	389.3	1.16	202
$SF_6 : C_2H_6 : He = 5 : 1 : 10$	1115	1.14	459.7	1.22	246
$SF_6 : C_2H_6 : Ne = 5 : 1 : 5$	1175	1.10	370.7	1.16	196.4

conditions of the experiment whose results are shown in Fig. 3 ($W_a = 0.13$ J cm^{-3} for $\tau > 3$ μs) were equal to 1400, 1310, and 1250 K in the mixtures of composition $SF_6 : C_2H_6 = 5 : 1$, $SF_6 : C_2H_6 : He = 5 : 1 : 5$ and $5 : 1 : 10$, respectively.

4.2 Structure and parameters of gas-dynamic perturbation region

The temperature jump at the boundary of irradiation region leads, as noted above, to the corresponding pressure difference, resulting in the generation of a shock wave propagating towards the cold gas. At the early stage of perturbation development, the boundaries exert no effect and the process is self-similar in character [16, 17]. Furthermore, the transverse dimensions of the perturbation region are far greater than the longitudinal ones, which permits considering the gas motion in a one-dimensional approximation. In view of the aforesaid and in accordance with Refs [16, 17], the shock-induced perturbation structure can be diagrammed schematically (Fig. 8). The shock front propagates into the unirradiated gas region denoted by the figure 0. Shock-compressed gas region 1 behind the front borders on rarefied gas region 2, which has experienced rarefaction wave 3. On the right the rarefaction wave is adjacent to region 4 of the unperturbed gas with a temperature T heated by the laser beam (see Section 4.1). The arrows in Fig. 8 indicate the direction of propagation of the shock wave, tangential discontinuity 1–2, and weak discontinuities 2–3 and 3–4.

On the basis of theoretical concepts developed in Refs [16, 17], the following system of equations can be written for determining the shock velocity V_{sh}:

$$\frac{p}{p_0}\left(1 - \frac{\gamma - 1}{2}\frac{U}{V_{s0}}\right)^{2\gamma/(\gamma-1)} = \frac{2\gamma_0 M_0^2 - (\gamma_0 - 1)}{\gamma_0 + 1}, \qquad (5)$$

$$U = M_0 V_{s0}\frac{2(M_0^2 - 1)}{M_0^2(\gamma_0 + 1)}, \quad M_0 = V_{sh}/V_{s0}. \qquad (6)$$

Here, U is the travelling velocity of the contact surface between the regions of compression 1 and rarefaction 2; M_0 is the Mach number. Since, as noted above, the gas density in region 4 is $\rho = \rho_0$, the shock-initiating pressure difference $\Delta p = p - p_0$ arises exclusively from the temperature jump $\Delta T = T - T_0$. The latter in turn is completely defined by the W_a value. Therefore, from Eqns (5) and (6) it follows that the shock velocity V_{sh} and the velocity U of the interface between regions 1 and 2 are functions of only the quantity W_a for given initial gas parameters. In view of this, all thermodynamic gas parameters in regions 1–3 are unambiguously determined by W_a.

Table 2 shows the values of V_{sh}, U, and thermodynamic parameters in the regions of gas compression 1 and rarefaction 2 for the four mixtures investigated in our work. The data were calculated with the use of Eqns (5) and (6), the data of Table 1, and the well-known relations of the theory of shock waves and self-similar motion in a polytropic gas [16, 17]. The values of p_2 are not given, because $p_2 = p_1$. Also given for comparison are the experimental values of V_{sh} measured from the dependences of the transverse dimension of a diffuse SSVD strip (see Figs 5–7) on τ. From Table 2 it follows that the values of T_1 are little different from T_0 and the values of T_2 are close to T. This testifies to the validity of our assumption that the adiabatic exponents γ and γ_0 should be treated as constants in the derivation of Eqns (5) and (6). One can also see that there is good agreement between the calculated and measured values of V_{sh}.

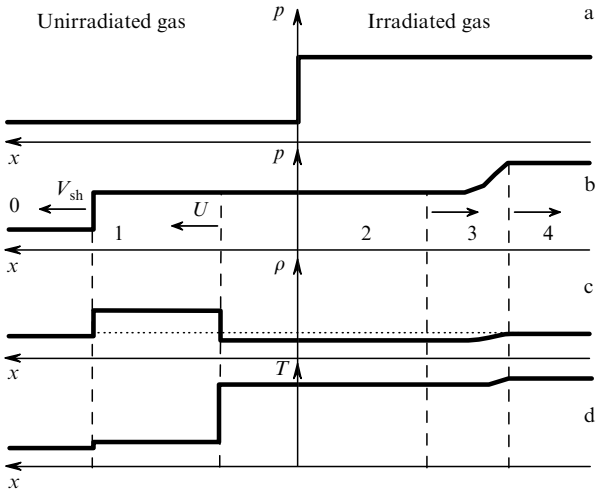

Figure 8. Perturbation structure: initial pressure jump (a) and the subsequent time evolution of the gas pressure p (b), density ρ (c), and temperature T (d).

4.3 Effect of gas-dynamic perturbations on discharge characteristics and SSVD structure.

The nature of gas-dynamic perturbation which occurs in SF_6-based mixtures in the absorption of CO_2-laser radiation allows us to gain a rather distinct impression of the features of SSVD development when the laser beam is profiled with a diaphragm or a screen. In general terms it reduces to the following. The 'whiskers', through which the current flows simultaneously with the initial SSVD current, are formed in regions 2 and 3 with a lowered gas density. The dark regions, which separate the 'whiskers' and the diffuse strip in the photographs in Figs 5 and 6, are located in regions 1 of the shock-compressed gas, while the narrowing of the diffuse discharge strip with τ is caused by the propagation of the shock wave front. The discharge therefore is a peculiar kind of shock wave visualiser.

Table 2. Values of V_{sh}, U, and thermodynamic parameters in the regions of compression 1 and rarefaction 2 (see Fig. 8) for $W_a = 0.11$ J cm^{-3} for different mixtures.

Mixture composition	V_{sh}/m s^{-1}		U/m s^{-1}	p/p_0	p_1/p_0	ρ_1/ρ_0	T_1/T_0	ρ_2/ρ_0	T_2/T_0
	Calculation	Experiment							
$SF_6 : C_2H_6 = 5 : 1$	230.7	240 ± 25	131.7	4.13	2.56	2.33	1.10	0.64	4.02
$SF_6 : C_2H_6 : He = 5 : 1 : 5$	311.1	310 ± 30	165.1	3.92	2.45	2.15	1.15	0.65	3.75
$SF_6 : C_2H_6 : He = 5 : 1 : 10$	366.5	360 ± 35	181.7	3.72	2.34	1.98	1.18	0.67	3.51
$SF_6 : C_2H_6 : Ne = 5 : 1 : 5$	296.3	320 ± 30	157.1	3.92	2.45	2.15	1.15	0.65	3.75

Let us discuss in greater detail the $\Delta(\tau)$ dependence represented in Fig. 3. By obvious symmetry about the central line of the electric field it would suffice to consider the gas perturbation structure in only one half of the discharge gap. For definiteness, we select the domain to the left of the gap symmetry axis. The distribution of the main thermodynamic gas parameters along the x axis, which is aligned with the travelling direction of the front of the side shock wave, may be pictorially represented with the help of Fig. 8 by bringing the ordinate axis into coincidence with the vertical boundary of irradiation region. One can see that rarefaction wave 3 and rarefaction region 2 are 'drawn' into the gap. This process is accompanied with the partial transfer of the discharge current to the periphery and the emergence of vertically directed lengths of the 'whiskers'.

The pressure jump caused by CO_2-laser gas heating is also responsible for the emergence of a shock wave travelling in the direction perpendicular to the travelling direction of the side shock waves. As a result, near the cathode there appear brightly glowing discharge parts in the regions with a lowered gas density, which are almost perpendicular to the central field line. For some period of time (which depends on the ratio between the transverse dimensions of the discharge at the anode in the irradiated gas and the irradiation region), beginning from the point in time when the energy of the laser pulse has already been introduced into the gas but a single channel with a heightened conductivity has not yet formed in the rarefaction regions located at the boundaries, the voltage across the gap remains invariable [the 'shelf' in the $\Delta(\tau)$ dependence in Fig. 3].

Upon the development of gap enveloping through channels ('whiskers'), which develop in the regions with a lowered gas density, the discharge shifts to this domain completely. In the lowered-density regions, the gas is in a vibrationally excited state, its temperature being hardly different from the temperature in region 4 of the irradiated gas at rest (see Table 2 and Fig. 8). That is why the critical values of reduced field intensity $(E/N)_{cr}$, whereby the ionisation rate is balanced out by the rate of electron attachment to the SF_6 molecules, are also approximately equal in the above regions. However, because of the lowered gas density in the region of 'whisker' development, the field intensity E_{cr} is below its magnitude in the irradiated unperturbed gas. As the rarefaction waves propagate into the gap, the length of the channels ('whiskers') and the voltage across the gap decreases. As a result, there appears a decreasing part in the $\Delta(\tau)$ dependence for sufficiently long delay times τ. For very long delay times, the quantity Δ may even become negative. In particular, for the mixture of composition $SF_6 : C_2H_6 : He = 5 : 1 : 5$ ($W_a = 0.13$ J cm^{-3}), the values of τ such that the parameter Δ passes through the zero are equal to about ~ 10 and ~ 43 μs when the transverse dimension of irradiation region is limited by the diaphragm and in the absence of beam diaphragming.

5. Conclusions

A good agreement between the calculated and measured shock wave velocities obtained in the present work is indicative of a rather high accuracy of temperature estimates for the gas heated by CO_2-laser radiation. This supposedly permits employing the method of SSVD initiation in gases preliminarily heated by a pulsed laser for the determination of their electric-discharge characteristics at high temperatures. In particular, undeniably of interest is the determination of the temperature dependence of the critical reduced electric intensity $(E/N)_{cr}$ for SF_6 – a gas of considerable importance for electrophysical applications [18, 19].

Acknowledgements. This work was supported by the Russian Foundation for Basic Research (Grant Nos 05-08-33704 and 06-08-00568) and the Russian Science Support Foundation.

References

1. Belevtsev A.A., Firsov K.N., in *Entsiklopediya nizkotemperaturnoi plazmy* (Encyclopaedia of Low Temperature Plasma) (Moscow: Fizmatlit, 2005) Vol. XI-4, p. 761.
2. Borisov V.P., Burtsev V.V., Velikanov S.D., Voronov S.L., Voronin V.V., Zapol'skii A.F., Zolotov M.I., Kurillov G.A., Mishchenko G.M., Podavalov A.M., Selemir V.D., Urlin V.D., Frolov Yu.N., Tsiberov V.P. *Kvantovaya Elektron.*, **30**, 225 (2000) [*Quantum Electron.*, **30**, 225 (2000)].
3. Richeboeuf L., Pasquiers S., Legentil M., Puech V. *J. Phys. D: Appl. Phys.*, **31**, 373 (1998).
4. Apollonov V.V., Belevtsev A.A., Firsov K.N., Kazantsev S.Yu., Saifulin A.V. *Proc. SPIE Int. Soc. Opt. Eng.*, **4747**, 31 (2001).
5. Apollonov V.V., Belevtsev A.A., Kazantsev S.Yu., Saifullin A.V., Firsov K.N. *Kvantovaya Elektron.*, **30**, 207 (2000) [*Quantum Electron.*, **30**, 207 (2000)].
6. Apollonov V.V., Belevtsev A.A., Firsov K.N., Kazantsev S.Yu., Saifulin A.V. *Proc. XIV Int. Conf. on Gas Discharges and their Applications* (Glasgow, UK, 2000) p. 409.
7. Belevtsev A.A., Firsov K.N., Kazantsev S.Yu., Kononov I.G. *J. Phys. D: Appl. Phys.*, **37**, 1759 (2004).
8. Slovetskii D.I., Deryugin A.A., in *Khimiya plazmy* (Plasma Chemistry) Ed. by B.M. Smirnov (Moscow: Energoatomizdat, 1987) Vol. 13, p. 240.
9. Belevtsev A.A., Firsov K.N., Kazantsev S.Yu., Kononov I.G. *Proc. IV Int. Conf. on Plasma Physics and Plasma Technology* (Minsk, Belarus, 2003) Vol. 1, p. 27.
10. Belevtsev A.A., Firsov K.N., Kazantsev S.Yu., Kononov I.G. *Appl. Phys. B*, **82**, 455 (2006).
11. Taylor R.S., Apollonov V.V., Corkum P.B. *IEEE J. Quantum Electron.*, **16**, 314 (1980).
12. Velikhov E.P., Kovalev A.S., Rakhimov A.T. *Fizicheskie yavleniya v gazorazryadnoi plazme* (Physical Phenomena in Gas-Discharge Plasmas) (Moscow: Nauka, 1980).
13. Gordiets B.F., Osipov A.I., Shelepin L.A. *Kinetic Processes in Gases and Molecular Lasers* (New York: Gordon&Breach, 1987; Moscow: Nauka, 1980).
14. Chervy B., Gleizes A., Razafinimanana M. *J. Phys. D: Appl. Phys.*, **27**, 1193 (1994).
15. Grigor'ev I.S., Meilikhov E.Z. (Eds) *Fizicheskie Velichiny (Spravochnik)* (Handbook of Physical Quantities) (Moscow: Energoatomizdat, 1991).
16. Landau L.D., Lifshits E.M. *Fluid Mechanics* (Oxford: Pergamon Press, 1987).
17. Zel'dovich Ya.B., Raizer Yu.P. *Physics of Shock Waves and High-Temperature Hydrodynamic Phenomena* (New York: Acad. Press, 1966, 1967) Vols 1 and 2.
18. Datfkof P., Christophorou L., Carter J. *J. Chem. Phys.*, **99**, 8607 (1993).
19. Aleksandrov N.L., Bazelyan E.M., Konchakov A.M. *Fiz. Plazmy*, **29**, 182 (2003).